ELSEVIER

Available online at www.sciencedirect.com

SCIENCE DIRECT®

International Journal of Solids and Structures 43 (2006) 675–685

INTERNATIONAL JOURNAL OF SOLIDS and STRUCTURES

www.elsevier.com/locate/ijsolstr

Dynamic stability of electrostatic torsional actuators with van der Waals effect

Jian-Gang Guo, Ya-Pu Zhao *

State Key Laboratory of Nonlinear Mechanics (LNM), Institute of Mechanics, Chinese Academy of Sciences, Beijing 100080, People's Republic of China

Received 1 October 2004; received in revised form 31 March 2005
Available online 19 May 2005

Abstract

The influence of van der Waals (vdW) force on the stability of electrostatic torsional nano-electro-mechanical systems (NEMS) actuators is analyzed in the paper. The dependence of the critical tilting angle and voltage is investigated on the sizes of structure with the consideration of vdW effects. The pull-in phenomenon without the electrostatic torque is studied, and a critical pull-in gap is derived. A dimensionless equation of motion is presented, and the qualitative analysis of it shows that the equilibrium points of the corresponding autonomous system include center points, stable focus points, and unstable saddle points. The Hopf bifurcation points and fork bifurcation points also exist in the system. The phase portraits connecting these equilibrium points exhibit periodic orbits, heteroclinic orbits, as well as homoclinic orbits.

Keywords: Electrostatic torsional actuator; van der Waals force; Pull-in; Stability; Bifurcation; Periodic orbit; Heteroclinic orbit; Homoclinic orbit

1. Introduction

The van der Waals (vdW) interaction between two macroscopic bodies (spheres, film, plates etc.) has been widely investigated for nearly half a century (Lifshitz, 1956; Høye and Brevik, 1998; Boström and Sernelius, 2001; Kirsch, 2003). It became more emerging in recent years because of its profound theoretical background in the fields of atomic force microscopy (AFM), nano/micro-electro-mechanical-systems (NEMS/MEMS) devices, etc. The vdW force dominates the interaction between the probe of AFM and

* Corresponding author. Tel.: +86 10 6265 8008; fax: +86 10 6256 1284.
E-mail address: yzhao@lnm.imech.ac.cn (Y.-P. Zhao).

0020-7683/$ - see front matter © 2005 Elsevier Ltd. All rights reserved.
doi:10.1016/j.ijsolstr.2005.03.073

the sample (see Ashhab et al., 1999; Lee et al., 2002; Rützel et al., 2003), and plays an important role in NEMS structures (see Van Spengen et al., 2002; Buks and Roukes, 2001; Zhao et al., 2003; Lin and Zhao, 2003; Guo and Zhao, 2004). Ashhab et al. (1999) and Lee et al. (2002, 2003) built mathematical models by vdW potential to describe the interaction between the microcantilevers of AFM probe and the sample, and studied the bifurcation and chaos phenomena in the system. Influence of vdW effect and Casimir on the NEMS/MEMS behavior was investigated, and instability and adhesion in the NEMS/MEMS caused by vdW effects were also analyzed (Van Spengen et al., 2002; Buks and Roukes, 2001; Zhao et al., 2003; Lin and Zhao, 2003; Guo and Zhao, 2004; Chan et al., 2001). Chan et al. (2001) showed by experiments how the Casimir force can be used to actuate the MEMS devices. Zhao and his group studied the dynamic behavior of nano-scale electrostatic parallel-plate RF switches with the consideration of the vdW effects, and analyzed the bifurcation phenomena of the system (see Lin and Zhao, 2003). Zhao and his group also analyzed and compared the influence of van der Waals and Casimir forces on electrostatic torsional actuators in static equilibrium, and investigated the dependence of the critical tilting angle and pull-in voltage on the sizes of structure (see Guo and Zhao, 2004).

Electrostatic torsional actuators are important NEMS/MEMS devices, which are generally actuated by electrostatic forces. The schematic of a typical torsional actuator with rectangular section is shown in Fig. 1. A tilting angle φ is only freedom degree of the system (Fig. 2). The pull-in is an important phenomenon of electrostatic actuators, and the critical tilting angle and the pull-in voltage are characteristic quantities.

The pull-in analyses of the electrostatic torsional microactuators have been extensively reported in many literatures, and the analytical models have been derived for the calculation of the pull-in voltage and tilting angle. Satter et al. (2002) and Plötz et al. (2002) reported a new surface micromachined torsional actuator for integrated microswitches. The design and stability analysis of the actuator were also presented. Degani et al., 1998, 2002; Degani and Nemirovsky, 2004 and Nemirovsky and Degani (2001) proposed a pull-in polynomial algebraic equation for the pull-in angle and pull-in voltage of electrostatic actuator. The dependence of pull-in parameters on the design and properties of the actuator was also discussed. A lumped two-degrees-of-freedom pull-in model was taken into account (see Degani and Nemirovsky, 2004), and the experimental verification was also presented. Xiao et al. (2001, 2002, 2003) developed an angle-based design

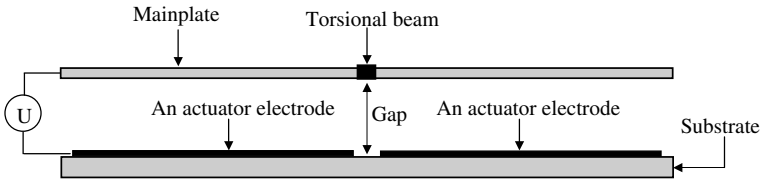

Fig. 1. Schematic side view of the torsional actuator.

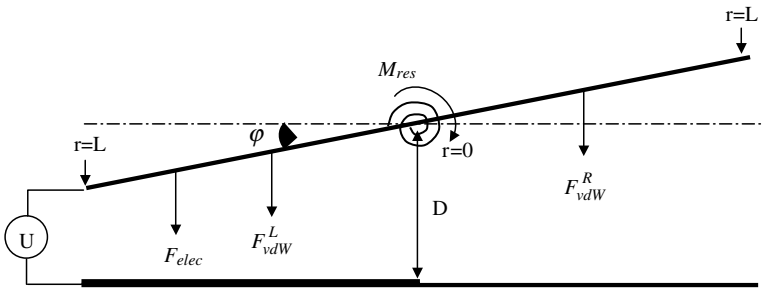

Fig. 2. 1DOF model of torsional actuator with vdW force.

approach for rectangular and round double-gimbaled electrostatic torsional actuators, and compared the results of theoretical calculation with those of numerical simulation and experiment. The electrostatic torsional mirror was also investigated from experiment and theory by some literatures (see Jaecklin et al., 1994; Toshiyoshi and Fujita, 1996; Zhang et al., 2001). However, the vdW or Casimir effects were not considered for the torsional actuators in these literatures, so the theoretical results of critical tilting angle and pull-in voltage were higher than experimental results. Though the authors of this paper investigated the influence of the vdW and Casimir effects on torsional actuators (see Guo and Zhao, 2004), however, only static equilibrium problem was considered. In fact, the instability is a dynamic process, and dynamic stability should be given more attention. To dynamic equilibrium problem, the inertial and damping effects will be included. In this paper, the simplified one-degree-of-freedom (1DOF) model is applied to study the dynamic stability of the electrostatic torsional NEMS actuator. The influence of vdW torque is investigated, and inertial and damping effects are simultaneously considered. Several kinds of driving torques and an elastic restoring torque are derived in Section 2. In Section 3, the dimensionless equations are derived, and the influence of vdW on the stability of torsional actuators is investigated. Moreover, the nonlinear equation of motion is analyzed qualitatively.

2. Theoretical model

The schematic of an electrostatic torsional actuator is shown in Fig. 1. In a first-order approximation, the mainplate of the device is considered to be a tiltable rigid body. Hence, the model has one-degree-of-freedom, and the angle of torsion φ is the only variable (shown in Fig. 2). When the voltage between one of the actuator electrodes and the mainplate is applied, an electrostatic attracting force between them will produce an electrostatic torque, and under the action of the torque, the mainplate will tilt. The electrostatic torque is expressed as (see Satter et al., 2002)

$$M_{\text{elec}} = \frac{1}{2}\varepsilon w U^2 \cdot \frac{1}{\sin^2\varphi}\left[\frac{D}{D - L\sin\varphi} - 1 + \log\left(\frac{D - L\sin\varphi}{D}\right)\right], \tag{1}$$

where ε denotes the electric permittivity, U the applied voltage, D the gap between torsional axis and bottom electrodes, and L, w and φ are the half-length, width and tilting angle of the mainplate, respectively.

Besides the electrostatic force, vdW force also plays an important role when the sizes of structure are sufficiently small. When two plates of torsional actuator keep parallel, i.e. $\varphi = 0$, the vdW force at the left of fixed axis equals to its counterpart at the right. The resultant torque of forces at both sides to the fixed axis is zero (Fig. 2). When the mainplate of actuator tilts, the vdW force at one side of fixed axis will not be equal to its counterpart at another side, and the resultant of vdW torque is not zero.

When the mainplate rotates anti-clockwise an angle φ, the vdW differential forces acting on parallel differential plates with width w and infinitesimal length dr at the both sides of torsional beam (see Guo and Zhao, 2004) are

$$\mathrm{d}F^{\mathrm{L}}_{\text{vdW}} = \frac{Aw}{6\pi}\cdot\frac{\mathrm{d}r}{(D + r\sin\varphi)^3}, \quad \mathrm{d}F^{\mathrm{R}}_{\text{vdW}} = \frac{Aw}{6\pi}\cdot\frac{\mathrm{d}r}{(D + r\sin\varphi)^3}, \tag{2}$$

where $A = \pi^2\alpha\rho^2$ is the Hamaker constant, which lies in the range $(0.4\text{–}4)\times 10^{-19}$ J, ρ (Table 1) is the volume density of material, and α is a constant character in the interactions between the two atoms. The torque of these vdW differential forces to fixed torsional beam is (see Guo and Zhao, 2004)

$$M_{\text{vdW}} = \int_0^L r\cdot(\mathrm{d}F^{\mathrm{L}}_{\text{vdW}} - \mathrm{d}F^{\mathrm{R}}_{\text{vdW}}) = \frac{Aw}{12\pi}\cdot\frac{1}{\sin^2\varphi}\left[\frac{D + 2L\sin\varphi}{(D + L\sin\varphi)^2} + \frac{-D + 2L\sin\varphi}{(-D + L\sin\varphi)^2}\right]. \tag{3}$$

Table 1
Parameters of numerical calculation

Class	Parameter		
	Items	Symbol	Value
Physical constant	Hamaker constant	A	$(0.4–4)\times10^{-19}$ J
	Shear modulus of polysilicon	G	6.6×10^{10} Pa
The movable plate	Length	L	10^{-4} m
	Width	w	10^{-4} m
Torsional beam	Length	l	6.5×10^{-5} m
	Width	B	1.55×10^{-6} m
	Thickness	a	1.5×10^{-6} m
The gap	Dimensionless gap	d	$(0–3)\times10^{-2}$

Due to $D/L \ll 1$, the tilting angle is small, and an approximation is used, i.e., $\sin\varphi \approx \varphi$. Therefore the maximum torsional angle is $\varphi_0 \approx \sin\varphi_0 = D/L$ (see Satter et al., 2002). A dimensionless quantity d can be introduced as $d = D/L$, so $\varphi_0 = d$. The physical meaning of d is the ratio of the gap between two plates to the half-length of mainplate. Furthermore, by introducing the normalized tilting angle $\gamma = \varphi/\varphi_0$, where the value of γ is evidently in the range of $[0,1)$, we rewrite Eqs. (1) and (3) as

$$M_{\text{elec}} = \frac{1}{2}\frac{\varepsilon w L^2 U^2}{D^2}\cdot\frac{1}{\gamma^2}\left[\frac{\gamma}{1-\gamma}+\log(1-\gamma)\right], \tag{4}$$

$$M_{\text{vdW}} = \frac{AwL^2}{3\pi D^3}\frac{\gamma}{(1-\gamma^2)^2}. \tag{5}$$

When the mainplate rotates around the torsional beam, a restoring torque, M_{res}, will be produced, which is caused by elastic restoring force of the beam. The system can be simplified as a flexure spring with torsional stiffness K. In addition, a damping torque and an inertia torque should also be considered. Three kinds of torques are expressed as (see Satter et al., 2002)

$$M_{\text{res}} = K\varphi = 2\frac{GJ_\rho D}{lL}\gamma, \tag{6}$$

$$M_{\text{damping}} = C\dot{\varphi} = \frac{CD}{L}\dot{\gamma}, \tag{7}$$

$$M_{\text{inertia}} = I\ddot{\varphi} = \frac{ID}{L}\ddot{\gamma}, \tag{8}$$

where G, J_ρ, l denote the shear modulus, the area moment of inertia and the length of torsional beam springs, and C and I are the effective damping constant and inertia moment of the mainplate, respectively. The dot above φ and γ denotes time derivative. The area moment of inertia,J_ρ, of the rectangular cross-section is expressed as (Zhang et al., 2001)

$$J_\rho = \begin{cases} ab^3\left[\frac{1}{3}-0.21\frac{b}{a}\left(1-\frac{b^4}{12a^4}\right)\right] & (b\leqslant a),\\ a^3b\left[\frac{1}{3}-0.21\frac{a}{b}\left(1-\frac{a^4}{12b^4}\right)\right] & (b\geqslant a), \end{cases} \tag{9}$$

where a and b are the thickness and the width of torsional beam, respectively. The effective damping constant, C, is a function of the torsion angle and can be calculated as (see Satter et al., 2002)

$$C = \frac{SL^2}{D^3}\frac{(1-\gamma^2)}{(1-\gamma^2)^2}, \tag{10}$$

where S is a constant depending on the geometry of the plate and the viscosity of the gas, and can be calibrated with reference to the experiment data.

3. Stability analysis of torsional actuators

The static equilibrium relation, $M_{\text{elec}} = M_{\text{res}}$, is given without the consideration of vdW effect. And a constant critical tilting angle $\gamma_{\text{cr}} \equiv 0.4404$ is derived (Satter et al., 2002; Degani et al., 1998; Degani and Nemirovsky, 2004; Xiao et al., 2003), and pull-in voltage could be calculated when the sizes of actuators are specified. The vdW torque is negligible in MEMS, but plays an important role in NEMS. When vdW torque is taken into consideration, the resultant of the electrostatic and the vdW torques reaches a balance with the elastic restoring torque of beam, and the static equilibrium relation accordingly becomes:

$$M_{\text{elec}} + M_{\text{vdW}} - M_{\text{res}} = 0. \tag{11}$$

Substituting Eqs. (4)–(6) into Eq. (11), a dimensionless equilibrium equation can be derived:

$$-\gamma + \mu \frac{1}{\gamma^2}\left[\frac{\gamma}{1-\gamma} + \log(1-\gamma)\right] + \beta \frac{\gamma}{(1-\gamma^2)^2} = 0, \tag{12}$$

where $\mu = \frac{\varepsilon w U^2}{2Kd^3}$ and $\beta = \frac{Aw}{3\pi KLd^4}$ are two dimensionless parameters denoting the ratios of the electrostatic and the vdW torques to the restoring torque, respectively.

The functional relation of applied voltage and tilting angle, $U = U(\gamma)$, can be derived via Eq. (12) (see Guo and Zhao, 2004). When the sizes of torsional actuators are specified, we can calculate the critical tilting angle γ_{cr} by $\mathrm{d}U/\mathrm{d}\gamma = 0$ (see Guo and Zhao, 2004). Substitute γ_{cr} into Eq. (12), and the pull-in voltage U_{cr} can be obtained (see Guo and Zhao, 2004). The values of critical tilting angle and pull-in voltage are dependent on the sizes of structures. The variation of γ_{cr} with the dimensionless gap d is shown in Fig. 3. It can be seen from Fig. 3 that the critical tilting angle does not keep constant 0.4404 but tends to the constant with the increase of the gap. The critical tilting angle reaches 0.4404 and does not increase until the dimensionless gap exceeds about 0.005.

Without the electrostatic torque, the pull-in can still occur with small angle perturbation because of the vdW effect. Let $\mu = 0$ in Eq. (12), we can obtain an expression of dimensionless gap $\mathrm{d}(\gamma)$. Then the critical gap can be derived as

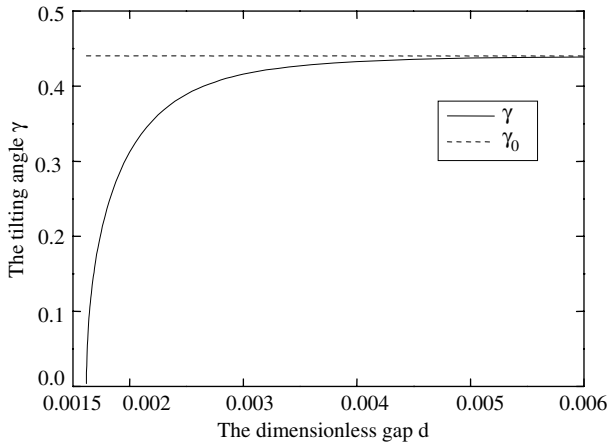

Fig. 3. Variation of the critical tilting angle with the dimensionless gap.

$$d_{\mathrm{cr}} = \lim_{\gamma\to 0}\left[\frac{Aw}{3\pi KL}\cdot\frac{1}{(1-\gamma^2)^2}\right]^{\frac{1}{4}} = \left(\frac{Aw}{3\pi KL}\right)^{\frac{1}{4}}. \tag{13}$$

When the inertial and damping effects are considered, the dimensionless equation of motion including vdW torque can be written as

$$\frac{\mathrm{d}^2\gamma}{\mathrm{d}\tau^2} + \eta\frac{\mathrm{d}\gamma}{\mathrm{d}\tau} + \omega\gamma = \xi\frac{1}{\gamma^2}\left(\frac{\gamma}{1-\gamma} + \log(1-\gamma)\right) + \delta\frac{\gamma}{(1-\gamma^2)^2}, \tag{14}$$

where the dimensionless quantities are $\eta = \frac{CT}{I}$, $\omega = \frac{KT^2}{I}$, $\xi = \frac{\varepsilon w T^2 U^2}{2Id^3}$, $\delta = \frac{AwT^2}{3\pi ILd^4}$ and $\tau = \frac{t}{T}$, and T is a characteristic time. Eq. (14) is a nonlinear ordinary differential equation. The qualitative analysis of the nonlinear equation is made below to obtain the whole properties of the solutions.

Setting $\frac{\mathrm{d}\gamma}{\mathrm{d}\tau} = \Theta$, Eq. (14) can be transformed into the following autonomous system

$$\begin{cases} \dfrac{\mathrm{d}\gamma}{\mathrm{d}\tau} = \Theta, \\ \dfrac{\mathrm{d}\Theta}{\mathrm{d}\tau} = -\eta\Theta - \omega\gamma + \xi\dfrac{1}{\gamma^2}\left(\dfrac{\gamma}{1-\gamma} + \log(1-\gamma)\right) + \delta\dfrac{\gamma}{(1-\gamma^2)^2}. \end{cases} \tag{15}$$

The Jacobian matrix of the autonomous system is

$$\begin{pmatrix} 0 & 1 \\ F'(\gamma) & -\eta \end{pmatrix}, \tag{16}$$

where

$$F(\gamma) = -\omega\gamma + \xi\frac{1}{\gamma^2}\left(\frac{\gamma}{1-\gamma} + \log(1-\gamma)\right) + \delta\frac{\gamma}{(1-\gamma^2)^2},$$

and the prime denotes the differential with respect to γ. The corresponding eigenvalues of the Jacobian matrix are $\lambda_{1,2} = \frac{1}{2}(-\eta \pm \sqrt{\eta^2 + 4F'(\gamma)})$.

In order to obtain the equilibrium states of the autonomous system, we have to solve the equation $F(\gamma) = 0$. And it is obvious that the equation $F(\gamma) = 0$ is exactly equivalent to Eq. (12), which is an implicit algebraic equation, and the voltage U in the dimensionless parameter ξ is the function of γ. To every value specified of U, the equation $F(\gamma) = 0$ has many real and complex roots, but only the real roots between 0 and 1 have physical meaning. The extreme value point $(\gamma_{\mathrm{cr}}, U_{\mathrm{cr}})$ can be calculated by solving the equation, $F'(\gamma) = 0$, where γ lies in the range of $[0, 1)$, and which is the same as static problem above. In addition, when the value of voltage U equals to zero, i.e. the dimensionless parameter $\xi = 0$, another critical value $d_{\mathrm{cr}} = (\frac{Aw}{3\pi KL})^{\frac{1}{4}}$ can be obtained by Eq. (13). Hence, according to the values of parameters U and d, we can discuss the equilibrium states of the autonomous system by following five cases.

(1) $d > d_{\mathrm{cr}}$ and $U < U_{\mathrm{cr}}$.

For the voltage $U < U_{\mathrm{cr}}$, the curve of function $F(\gamma)$ is given in Fig. 4 when the independent variable γ is in the range of $(0, 1)$. It can be shown from Fig. 4 that the curve has two points of intersection (γ_1 and γ_2) with the line $F = 0$, i.e., the equation $F(\gamma) = 0$ has two real roots between 0 and 1. So the autonomous system has two equilibrium points: $Q_1(\gamma_1, 0)$, $Q_2(\gamma_2, 0)$, and $\gamma_1 < \gamma_{\mathrm{cr}} < \gamma_2$, where γ_{cr} is the critical tilting angle calculated by $F'(\gamma) = 0$.

For equilibrium point Q_1, because of $F'(\gamma_1) < 0$, the eigenvalues of the Jacobian matrix are a couple of pure imaginary roots when the parameter $\eta = 0$, so it is a center point. When the parameter $\eta \neq 0$ and $\eta^2 < 4|F'(\gamma)|$, the eigenvalues of the Jacobian matrix are a couple of conjugate complex roots, so the equilibrium point Q_1 is a focus point. In general, there exists $\eta > 0$, so the real parts of the couple of conjugate

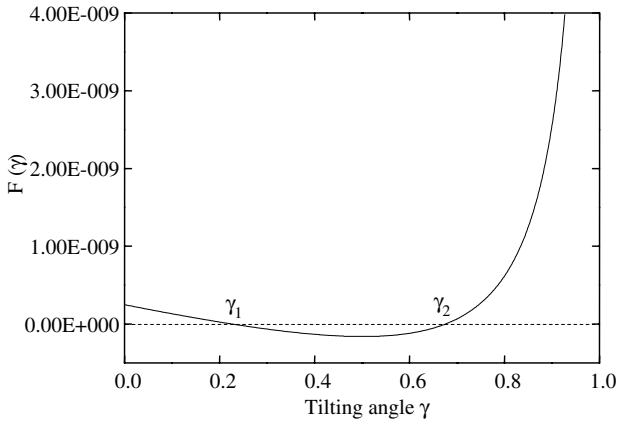

Fig. 4. Variation of $F(\gamma)$ with the critical tilting angle when the applied voltage $U = 5.5V < U_{cr}$.

complex roots are negative, and the focus point is stable. Likewise, when parameter $\eta \neq 0$ and $\eta^2 > 4|F'(\gamma)|$, the eigenvalues are two real roots with opposite signs, and the equilibrium point Q_1 is an unstable saddle point, however which is unreasonable for $U < U_{cr}$ in physical view, and the condition $\eta^2 < 4|F'(\gamma)|$ should be satisfied.

For equilibrium point Q_2, because of $F'(\gamma_2) > 0$, the eigenvalues are two real roots with opposite signs whether η is equal to zero or not. So Q_2 is an unstable saddle point. Hence, the phase portraits connecting Q_1, Q_2 on the phase plane include periodic, heteroclinic and homoclinic orbits (as shown in Figs. 5 and 6). When the damping is not considered, i.e. $\eta = 0$, the equilibrium point Q_1 is a center point, and there are periodic orbits around it and homoclinic orbits starting from Q_2 and going back to Q_2 (as shown in Fig. 5). It can be concluded that the movable plate makes periodic oscillation near the equilibrium point Q_1 and snaps down the substrate beyond the saddle point Q_2. When the damping is taken into account, i.e. $\eta \neq 0$, the equilibrium point Q_1 is a stable focus point, so there are heteroclinic orbits around it as well as saddle point Q_2 (as shown in Fig. 6). The movable plate makes convergent oscillation near the focus point Q_1 and snaps down the substrate beyond the saddle point Q_2 (as shown in Fig. 6).

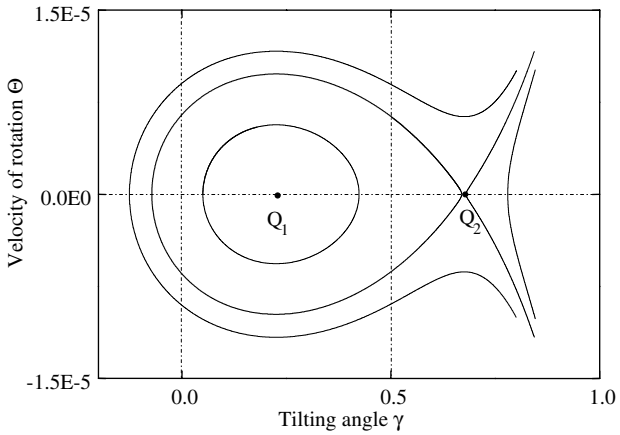

Fig. 5. The phase portrait on the phase plane of $\Theta - \gamma$ without the damping when the applied voltage $U = 5.5V < U_{cr}$ and the dimensionless gap $d > d_{cr}$.

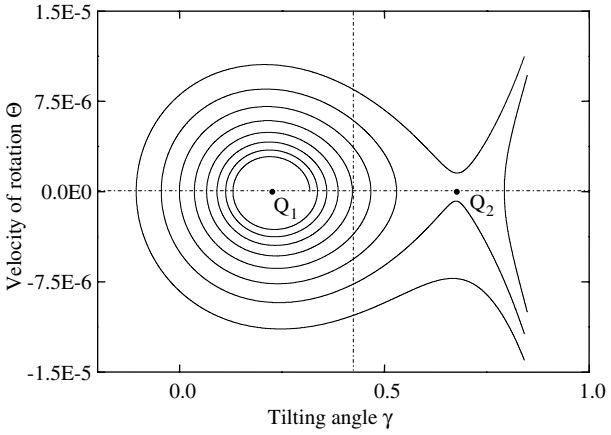

Fig. 6. The phase portrait on the phase plane of $\Theta - \gamma$ with the damping when the applied voltage $U = 5.5 < U_{cr}$ and the dimensionless gap $d > d_{cr}$.

In addition, to equilibrium point $(\gamma_1, 0; \eta)$, when the parameter η varies, there appears bifurcation. It has been known from the analysis above that the eigenvalues of the Jacobian matrix are a couple of pure imaginary roots when the parameter $\eta = 0$, and the real parts of the eigenvalues are positive if the parameter $\eta < 0$, and are negative if the parameter $\eta > 0$. The eigenvalues go across imaginary axis from the above or below of the complex plane ($\mathrm{Re}\,\lambda$, $\mathrm{Im}\,\lambda$). According to the eigenvalues criterion of bifurcation, the point $(\gamma_1, \Theta; \eta) = (\gamma_1, 0; 0)$ is a Hopf bifurcation.

(2) $d > d_{cr}$ and $U = U_{cr}$.

When the applied voltage U increases to U_{cr}, two points of intersection (γ_1 and γ_2) between the curve of $F(\gamma)$ and the line $F = 0$ tend towards and meet at the point $(\gamma_{cr}, 0)$. So the equation $F(\gamma) = 0$ has a single real root γ_{cr} between 0 and 1, particularly $\gamma_{cr} = 0.4404$ when $\delta = 0$, which simultaneously satisfies the equation the equation $F'(\gamma_1) = 0$. So the autonomous system has an equilibrium points $P(\gamma_{cr}, 0)$ when $U = U_{cr}$. The eigenvalues of Jacobian matrix are two repeated zero roots when the parameter $\eta = 0$, and a zero root and a nonzero real root when $\eta \neq 0$. In addition, the nonzero real root is negative if the parameter $\eta > 0$, and is positive if $\eta < 0$. So the equilibrium point $(\gamma, \Theta; \eta) = (\gamma_{cr}, 0; 0)$ is a fork bifurcation.

(3) $d > d_{cr}$ and $U = 0$ (without the electrostatic torque).

When the applied voltage $U = 0$, i.e., the dimensionless parameter $\xi = 0$, the function is reduced to $F(\gamma) = -\omega\gamma + \delta\frac{\gamma}{(1-\gamma^2)^2}$. When the dimensionless gap d is specified, the curve of function $F(\gamma)$ is given in Fig. 7 with the variable γ in the range of $[0, 1)$. It can be shown from Fig. 7 that the curve has two points of intersection ($\gamma_1 = 0$ and γ_2) with the line $F = 0$, i.e., the equation $F(\gamma) = 0$ has two real roots. So the autonomous system has two equilibrium points $Q_1(0, 0)$, $Q_2(\gamma_2, 0)$ in the region of $[0, 1)$, where γ_2 is the nonzero positive real root. However, due to the symmetric structure and antisymmetric torques of torsional actuators when $U = 0$, there exists another equilibrium point $Q_3(-\gamma_2, 0)$.

For equilibrium point Q_1, similar to the analysis of the first case, it is a center point when the parameter $\eta = 0$, and is a stable focus point when the parameter $\eta \neq 0$. It can be concluded that the movable plate makes convergent oscillation near the focus point because of the damping, and makes periodic oscillation if the damping is neglected. The equilibrium point Q_2 and Q_3 are unstable saddle points for any η. The phase orbits connecting three equilibrium points on the phase plane are shown in Figs. 8 and 9, which include the periodic, heteroclinic and homoclinic orbits. In addition, to equilibrium point Q_1, because the

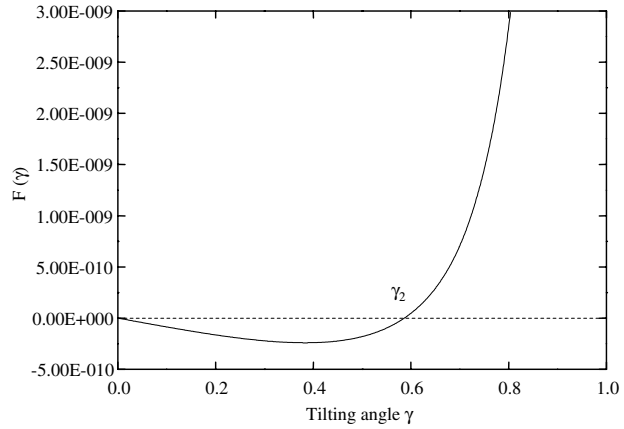

Fig. 7. Variation of $F(\gamma)$ with the critical tilting angle when the applied voltage $U = 0$ and the dimensionless gap $d = 2.0 \times 10^{-3} > d_{cr}$.

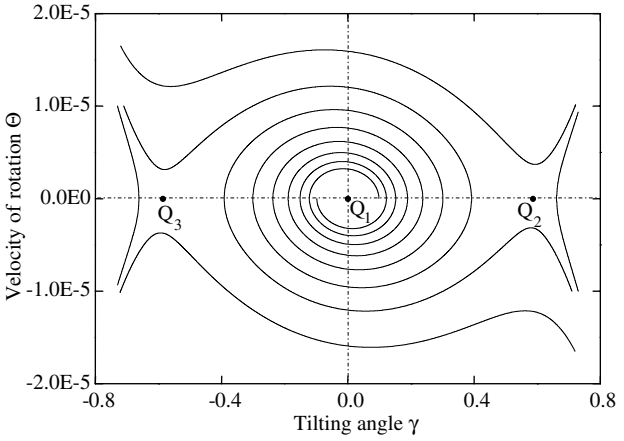

Fig. 8. The phase portrait on the phase plane of $\Theta - \gamma$ with the damping when the applied voltage $U = 0$ and the dimensionless gap $d > d_{cr}$.

eigenvalues of the Jacobian matrix are a couple of pure imaginary roots when the parameter $\eta = 0$, similar to the analysis in case 1, the point $(\gamma, \Theta; \eta) = (0, 0; 0)$ is a Hopf bifurcation point.

(4) $d = d_{cr}$ and $U = 0$.

When the dimensionless gap d approaches the critical value d_{cr}, the point of intersection Q_2 tends towards the point Q_1, and they finally converge at the point $Q_1(0, 0)$, which satisfies simultaneously the equation $F(\gamma) = -\omega\gamma + \delta\frac{\gamma}{(1-\gamma^2)^2} = 0$ and the equation $F'(\gamma) = 0$. The eigenvalues of corresponding Jacobian matrix are two repeated zero roots when the parameter $\eta = 0$, and a zero root and a nonzero real root when $\eta \neq 0$. In addition, the nonzero real root is negative if the parameter $\eta > 0$, and is positive if $\eta < 0$. So when the dimensionless gap d reaches critical value d_{cr}, the equilibrium point $(\gamma, \Theta; \eta) = (0, 0; 0)$ becomes a fork bifurcation.

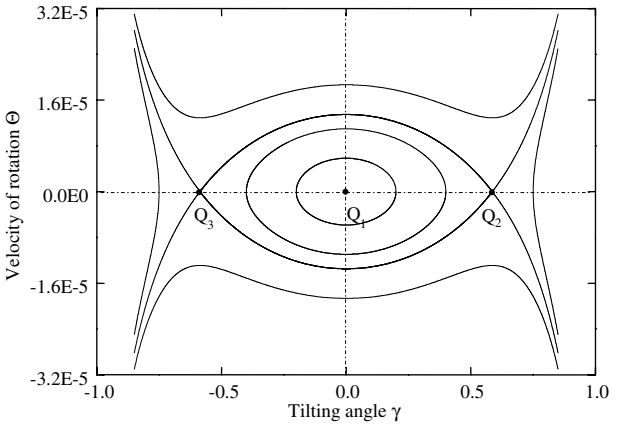

Fig. 9. The phase portrait on the phase plane of $\Theta - \gamma$ without the damping when the applied voltage $U = 0$ and the dimensionless gap $d > d_{cr}$.

(5) $d < d_{cr}$ or $U > U_{cr}$.

The pull-in will automatically happen when the gap is less than d_{cr} or the voltage greater than U_{cr}. So the autonomous system has no equilibrium point in the case.

The phase portraits (Figs. 5, 6, 8, 9) show the overall properties of solutions, and the further analyses of the nonlinear differential equation can be made on the basis of the present paper. The bifurcation points of the system are obtained, which are important for dynamic analyses of nonlinear systems. In addition, it is possible for chaos to exist in torsional NEMS actuators when the vdW and other surface effects are considered.

4. Conclusion

The dimensionless equilibrium equations of electrostatic torsional actuators are presented with the consideration of the vdW torque in the paper. With the vdW effect, the inherent instability of the actuators is dependent on the scales of structures. The critical tilting angle approximately keeps constant only in micron or larger scales, but it is not constant when the gap between two plates is in nano-scales. The pull-in voltage is also lower than that without consideration of vdW torque. Without the electrostatic torque, the pull-in can still occur with small angle perturbation, and a critical gap is derived. Furthermore, the qualitative analysis of the equation of motion shows that the equilibrium points of the corresponding autonomous system include stable focus point and center points, as well as unstable saddle points. The Hopf bifurcation points and fork bifurcation points also exist in the system. The phase portraits show the periodic, heteroclinic and homoclinic orbits.

Acknowledgements

The authors acknowledge the financial support of Chinese Academy of Sciences (No. KJCX2-SW-L2) and the National Natural Science Foundation of China (Grant Nos. 10225209, 50131160739 and 90305020).

References

Ashhab, M., Salapaka, M.V., Dahleh, M., Mezić, I., 1999. Dynamical analysis and control of microcantilevers. Automatica 35, 1663–1670.

Boström, M., Sernelius, B.E., 2001. Fractional van der Waals interaction between thin metallic films. Physical Review B 61, 2204–2210.

Buks, E., Roukes, M.L., 2001. Stiction, adhesion energy, and the Casimir effect in micromechanical systems. Physical Review B 63, 033402.

Chan, H.B., Aksyuk, V.A., Kleiman, R.N., Bishop, D.J., Capasso, F., 2001. Quantum mechanical actuation of microelectromechanical systems by the Casimir force. Science 291, 194–197.

Degani, O., et al., 1998. Pull-in study of an electrostatic torsion microactuator. Journal of Microelectromechanical Systems 7, 373–379.

Degani, O., Nemirovsky, Y., 2002. Design considerations of rectangular electrostatic torsion actuators based on new analytical pull-in expressions. Journal of Microelectromechanical Systems 11, 20–26.

Degani, O., Nemirovsky, Y., 2004. Experimental verification of a design methodology for torsion actuators based on a rapid pull-in solver. Journal of Microelectromechanical Systems 13, 121–130.

Guo, J.G., Zhao, Y.P., 2004. Influence of van der Waals and Casimir forces on electrostatic torsional actuators. Journal of Microelectromechanical Systems 13, 1027–1035.

Høye, J.S., Brevik, I., 1998. Van der Waals force between dielectric plates derived from the quantum statistical mechanical path integral method. Physica A 259, 165–182.

Jaecklin, V.P., et al., 1994. Line-addressable torsional micromirrors for light modulator arrays. Sensors and Actuators A 41/42, 324–329.

Kirsch, V.A., 2003. Calculation of the van der Waals force between a spherical particle and an infinite cylinder. Advances in Colloid and Interface Science 104, 311–324.

Lee, S.I., Howell, S.W., Raman, A., Reifenberger, R., 2002. Nonlinear dynamics of microcantilevers in tapping mode atomic force microscopy: A comparison between theory and experiment. Physical Review B 66 (115409), 1–10.

Lifshitz, E.M., 1956. The theory of molecular attractive forces between solids. Soviet Physics—JETP 2, 73–83.

Lin, W.H., Zhao, Y.P., 2003. Dynamics behavior of nanoscale electrostatic actuators. Chinese Physics Letter 20, 2070–2073.

Nemirovsky, Y., Degani, O., 2001. A methodology and model for the pull-in parameters of electrostatic actuators. Journal of Microelectromechanical Systems 10, 601–615.

Plötz, F., et al., 2002. A low-voltage torsional actuator for application in RF-microswitches. Sensors and Actuators A 92, 312–317.

Rützel, S., Lee, S.I., Raman, A., 2003. Nonlinear dynamics of atomic-force-microscopy probes driven in Lennard-Jones potentials. Proceedings of the Royal Society of London A 459 (2036), 1925–1948.

Satter, R., Plötz, F., Fattinger, G., Wachutka, G., 2002. Modeling of an electrostatics torsional actuator: demonstrated with an RF MEMS switch. Sensors and Actuators A 97–98, 337–346.

Toshiyoshi, H., Fujita, H., 1996. Electrostatic microtorsion mirrors for an optical switch matrix. Journal of Microelectromechanical Systems 5, 231–237.

Van Spengen, W.M., Puers, R., De Wolf, I., 2002. A physical model to predict stiction in MEMS. Journal of Micromechanics and Microengineering 12, 702–713.

Xiao, Z.X., Wu, X.T., Peng, W.Y., Farmer, K.R., 2001. An angle-based design approach for rectangular electrostatic torsion actuators. Journal of Microelectromechanical Systems 10, 561–568.

Xiao, Z.X., Wu, X.T., Peng, W.Y., Farmer, K.R., 2002. Pull-in study for round double-gimbaled electrostatic torsion actuators. Journal of Micromechanics and Microengineering 12, 77–81.

Xiao, Z.X., Wu, X.T., Peng, W.Y., Farmer, K.R., 2003. Analytical behavior of rectangular electrostatic torsion actuators with nonlinear spring bending. Journal of Microelectromechanical Systems 12, 929–936.

Zhang, X.M., et al., 2001. A study of the static characteristics of a torsional micromirror. Sensors and Actuators A 90, 73–81.

Zhao, Y.P., Wang, L.S., Yu, T.X., 2003. Mechanics of adhesion in MEMS—a review. Journal of Adhesion Science and Technology 17, 519–546.